Appendix to Peniston JH, Barfield M, Gonzalez A, Holt RD. Environmental Fluctuations can promote evolutionary rescue in high-extinction-risk scenarios. *Proceedings of the Royal Society B: Biological Sciences.* (doi:10.1098/rspb.2020.1144)

Generating autocorrelated Gaussian sequences

Equations (2.2) and (2.3a) were used to generate autocorrelated Gaussian sequences. Equation (2.2) is

$$\theta_{t+1} = \mu_\theta + \rho[\theta_t - \mu_\theta] + \sigma_\theta\sqrt{1-\rho^2}\eta_t .$$

If θ_t is a Gaussian with mean μ_θ and variance σ_θ^2, the right side is the sum of two Gaussians and is therefore Gaussian. The expected value of θ_{t+1} is

$$\begin{aligned} E\{\theta_{t+1}\} &= E\{\mu_\theta + \rho[\theta_t - \mu_\theta] + \sigma_\theta\sqrt{1-\rho^2}\eta_t\} \\ &= \mu_\theta + \rho[E\{\theta_t\} - \mu_\theta] + \sigma_\theta\sqrt{1-\rho^2}E\{\eta_t\} = \mu_\theta \end{aligned},$$

because $E\{\theta_t\} = \mu_\theta$ and $E\{\eta_t\} = 0$. The variance of θ_{t+1} is

$$\begin{aligned} &E\{(\theta_{t+1} - \mu_\theta)^2\} = E\{(\rho[\theta_t - \mu_\theta] + \sigma_\theta\sqrt{1-\rho^2}\eta_t)^2\} \\ &= \rho^2 E\{[\theta_t - \mu_\theta]^2\} + 2\rho\sigma_\theta\sqrt{1-\rho^2}E\{[\theta_t - \mu_\theta]\eta_t\} + \sigma_\theta^2(1-\rho^2)E\{\eta_t^2\} . \\ &= \rho^2\sigma_\theta^2 + 2\rho\sigma_\theta\sqrt{1-\rho^2}E\{[\theta_t - \mu_\theta]\}E\{\eta_t\} + \sigma_\theta^2(1-\rho^2) = \sigma_\theta^2 \end{aligned}$$

Finally, the correlation coefficent between θ_{t+1} and θ_t is

$$\begin{aligned} &E\{(\theta_t - \mu_\theta)(\theta_{t+1} - \mu_\theta)\}/\sigma_\theta^2 = E\{(\theta_t - \mu_\theta)(\rho[\theta_t - \mu_\theta] + \sigma_\theta\sqrt{1-\rho^2}\eta_t)\}/\sigma_\theta^2 \\ &= \rho E\{(\theta_t - \mu_\theta)^2\}/\sigma_\theta^2 + \sigma_\theta\sqrt{1-\rho^2}E\{(\theta_t - \mu_\theta)\eta_t\}/\sigma_\theta^2 = \rho \end{aligned} .$$

Therefore, if θ_t is Gaussian with mean μ_θ and variance σ_θ^2, so is θ_{t+1}, with a correlation coefficient between them of ρ. This can be assured by starting the sequence (θ_1) with a Gaussian with mean μ_θ and variance σ_θ^2. The same derivation of course applies to equation (2.3a).

However, for our simulations, we started the sequence with the mean value μ_θ. We made this choice because the effects of the initial degree of environmental change are well known and we were focused on the effects of variation afterwards. If the starting value is a random value drawn from a Gaussian, some of the effects of environmental variation could be just because there was variation in the degree of enviornmental change populations were exposed to. The drawback of our assumption is that equations (2.2) and (2.3a) no longer have the proper statistics. By starting the sequence at μ_θ, the initial variance of the sequence is 0. One generation later, the variance is $\sigma^2(1-\rho^2)$ and *t* generations later, the variance is $\sigma^2(1-\rho^{2t})$. The sequence is Gaussian with the proper mean, and this shows the variance approaches σ^2; it can also be shown that the correlation coefficient approaches ρ at the same time. So eventually the process has the statistics indicated, but if ρ is close to 1, it will take some time.

Starting the sequence with μ_θ or with a Gaussian random variable with mean μ_θ and variance σ_θ^2 does not seem to change the qualitative conclusions of our results. Therefore, as mentioned above, we decided to focus on the case with the sequence starting at μ_θ because we believe it more accurately reflects the effect of variation after the environmental change. Figure A13A–B shows results of the population-level polygenic simulations with the sequence starting with a Gaussian variable, which can be compared to the results in figure 2. The one case where this assumption does change results is that the benefits of increasing autocorrelation for high-extinction-risk populations no longer go away at very high levels of autocorrelation (compare figure A5 to A13C–D).

Polygenic individual-based simulations methods

These simulations kept track of individuals in a population exposed to an abrupt environmental change. Each individual had a genotypic value that was determined by 10 freely recombining, additive diploid loci. An individual's phenotype z was the sum of these loci plus a random environmental component drawn from a zero-mean, unit-variance Gaussian distribution. An individual with phenotype z survived to adulthood with probability $\exp\left[-(z-\theta_t)^2/(2\omega^2)\right]$, where θ_t is the optimal phenotype and ω determines the strength of selection. Population size was regulated by the number of available mating sites ('ceiling' density dependence). If more than *K* individuals survived to adulthood, *K* adults were randomly selected (without replacement) to occupy mating sites. For each individual occupying a mating site, a mate was randomly selected (with replacement) from all surviving adults (selfing was possible). Each mating pair produced F_t offspring. If fewer than *K* individuals survived to adulthood every individual occupied a mating site. After reproduction, all adults died.

Each locus in the offspring's genotype was determined by randomly choosing one allele from each parent at that locus. A mutation occurred on each haplotype with probability 0.01. When a mutation occurred, a random value drawn from a zero-mean Gaussian distribution with variance 0.05 was added to the previous value at a randomly selected allele on the haplotype.

As with the population-level simulations, we varied either the optimal phenotype or the mean population fecundity over time following equations (2.2) and (2.3a–b), respectively. Because each mating pair must produce an integer number of offspring, we had to round non-integer values. For any given mating pair, with probability $p_F = F_t - \text{trunc}(F_t)$, where trunc($F_t$) is the largest integer $\leq F_t$, the number of offspring produced was the mean population fecundity rounded up, and with probability $1-p_F$, it was rounded down. Therefore, if $F_t = 4.2$, with probability 0.2 the mating pair would produce 5 offspring and with probability 0.8 it would

produce 4 offspring. This method kept the expected number of offspring produced per mating pair each generation equal to F_t, while adding the minimum amount of additional demographic stochasticity.

Simulations were initiated with 1,000 offspring in the population. Initial genotypes were assigned by randomly selecting allelic values from a zero-mean Gaussian distribution with a variance equal to the stochastic house-of-cards approximation given by equation (14) in Bürger and Lynch (1995). We first simulated dynamics for 1,000 generations with a fixed optimal phenotype of 0 and fixed fecundity of μ_F. At generation 1,000, the optimal phenotype switched to μ_θ. The simulation then continued for another 1,000 generations during which either θ_t or F_t was varied. Finally, to evaluate whether or not the population was adapted, there was then a 200 generation assay period during which θ_t and F_t were fixed at μ_θ and μ_F, respectively. If the population persisted at the end of this period, we considered it adapted.

Monogenic simulation methods

Simulations were started with N^* non-mutants and no mutants, and the number of each type was tracked each generation. To generate the per capita fecundity each generation, a Gaussian random sequence was generated using equation (2.3a–b). The number of births to each adult had a Poisson distribution with this mean, so the number of births of each type (mutants and non-mutants) was determined by drawing a Poisson random deviate with mean equal to product of the fecundity and the number of adults of that type (the sum of Poisson random variables is also a Poisson). The number of mutations (new mutants) was binomially distributed given the number of non-mutant births and mutation rate, and was subtracted from the number of non-mutants and added to the mutants. The number of each type surviving to adulthood was then

binomially distributed given its juvenile number and survival probability. Each realization was continued until the population was extinct, the number of mutants reached 1,000, or 1,000 generations had passed. The probability of persistence was the fraction of 1,000,000 realizations for which the population was non-zero at the end.

Monogenic analytical model method

Let u be the probability of mutation, which produces a mutant offspring from a non-mutant parent. The fecundity for both mutants and non-mutants is F_t (which varies with t) and the survival probability of non-mutants is V and of mutants is v (both constant). The expected number of surviving offspring of a non-mutant is F_tV, the geometric mean of which is less than 1 (i.e. the non-mutant population is maladapted and faces extinction). For a mutant, the expected number of surviving offspring is F_tv, the geometric mean of which is greater than 1. If the number of offspring of each individual has a Poisson distribution with mean F_t, and survival of each offspring is independent of all others, the number of surviving offspring of each non-mutant or mutant also has a Poisson distribution with the mean F_tV or F_tv, respectively.

The initial population consists only of non-mutants, the number of which is expected to decline to 0. Evolutionary rescue requires the generation of at least one mutant whose lineage persists (i.e. is not lost to demographic stochasticity before becoming common). The expected number of mutants generated is the product of the mutation rate and the expected number of births to non-mutants before they go extinct. The probability of survival of the lineage of each mutant can be found using a branching process. Combining these values can give an estimate of the probability of rescue.

First, we will find the expected number of mutants produced before non-mutant extinction (mutation rate times expected number of births to non-mutants). The expected number of births is the expected value of the product of the population size and fecundity. The non-mutant population recursion is

$$N_{t+1} = F_t V N_t, \tag{A1}$$

where N_t is the number of adults in generation t, implying

$$N_t = N^* \prod_{j=1}^{t-1} (F_j V), \; t > 1, \tag{A2}$$

where $N_1 = N^*$ is the initial population size.

The expected value of the number of births in generation t is

$$E[F_t N_t] = N^* V^{-1} E[\prod_{j=1}^{t} (F_j V)]. \tag{A3}$$

The expected total number of births through generation t is then

$$E[\sum_{i=1}^{t} F_i N_i] = N^* V^{-1} \sum_{i=1}^{t} E[\prod_{j=1}^{i} (F_j V)]. \tag{A4}$$

To incorporate variation, we assumed that F_t varies with time. To simplify the analysis, we let $F_t V = \exp\{r_t\}$, where r_t is a Gaussian random sequence with mean m and standard deviation σ, and with values of r_t separated by g generations having correlation coefficient ρ^g. The geometric mean of $F_t V = \exp\{m\}$, so $m < 0$ is required for non-mutants to be maladapted. The product of $F_j V$ in equation (A4) is therefore the exponentiation of the sum of the corresponding values of r_j. The sum of Gaussians is itself Gaussian, so the product in equation (A4) has a lognormal distribution, which has an expected value of $\exp\{m_s + \sigma_s^2 / 2\}$, where m_s

and σ_s^2 are the mean and standard deviation of the Gaussian in the exponent, which is in this case the sum of i values of r_t . F_tV itself is lognormal at every time with $E[F_tV] = \exp\{m + \sigma^2/2\}$. Note that because V is constant, the statistics of F_t are identical to those of F_tV except for the scaling factor V, which causes a shift in the mean (but no change in σ or ρ) , so that the mean fecundity $\mu_f = m - \ln(V)$.

The mean of a sum is the sum of the means, and the means of r_t are all m. The variance of a sum is the sum of the variances plus twice the sum of the covariance of each pair of values. Each r_t has a variance of σ^2, and a pair of values separated by g generations has covariance $\rho^g\sigma^2$. The product in equation (A4) for the ith term of the summation has i terms, so

$$m_s = im, \tag{A5}$$

$$\sigma_s^2 = \sigma^2[i + 2\sum_{j=1}^{i-1}(i-j)\rho^j]. \tag{A6}$$

If the sequence is uncorrelated, then equation (A6) becomes $\sigma_s^2 = i\sigma^2$. Substituting this and equation (A5) into equation (A4) and taking the limit as t goes to infinity gives the total expected number of births

$$E[\sum_{i=1}^{\infty} F_i N_i] = N^* V^{-1} \frac{\exp\{m + \sigma^2/2\}}{1 - \exp\{m + \sigma^2/2\}} \tag{A7}$$

assuming $m + \sigma^2/2 < 0$ so the series converges (note that $m < 0$ guarantees that with no mutations the population will go extinct, but it can still have an infinite expected number of births before extinction if the series does not converge). The expected number of mutants is the product of the expected number of births in equation (A7) and u. However, the mutant survives to adulthood with probability v. Therefore, the expected total number of mutants that arise and survive to adulthood is given by

$$E[\sum_{i=1}^{\infty} vuF_i N_i] = \frac{vuN^*}{V} \frac{\exp\{m+\sigma^2/2\}}{1-\exp\{m+\sigma^2/2\}}. \quad \text{(A8)}$$

If there is no variation (so F_t is constant at $F = \exp\{m\}/V$), $\sigma = 0$ and the number of mutants is

$$E[\sum_{i=1}^{\infty} vuF_i N_i] = \frac{vuN^*F}{1-FV}. \quad \text{(A9)}$$

If the sequence (of r_t and therefore F_t) is correlated, then the series in equation (A4) is not geometric, and therefore there is no closed form solution. The first few terms of the expected number of births is

$$E[\sum_{i=1}^{t} F_i N_i] = \frac{N^*}{V}\left\{e^{m+\sigma^2/2} + e^{2m+\sigma^2[2+2\rho]/2} + e^{3m+\sigma^2[3+2(2\rho+\rho^2)]/2} + e^{4m+\sigma^2[4+2(3\rho+2\rho^2+\rho^3)]/2} \ldots\right\} \quad \text{(A10)}$$

The first term in brackets is due to births from the initial population, which is N^* multiplied by $E\{F_1\}$. The second term is for births in the following generation, which is proportional to the product of F_1 and F_2, with ρ being the correlation coefficient between the corresponding values of r_t, which inflates the variance (if positive). The third term is for the births in the third generation, which depends on the product of three consecutive values of F_t, which consists of two pairs with an underlying correlation of ρ and one pair (the first and last) with a correlation of ρ^2. This pattern continues, so that for the k^{th} term, there are $k-1$ pairs of r_t with a correlation of ρ, and then one fewer for each higher power of ρ, until there is just one pair with correlation ρ^{k-1}. After enough terms are included so that $\rho^i \approx 0$, the remaining part of the summation in brackets in equation (A10) is geometric, which for convergence requires $\sigma^2 < -2m(1-\rho)/(1+\rho)$ (recall that $m<0$). A higher variance than this limit results in an infinite mean number of births. For positive autocorrelation, the limit on σ^2 is less than the limit for an uncorrelated sequence.

Since it has no closed-form solution, equation (A10) must be solved numerically. Results of this computation as a function of σ for $\rho = 0$ and 0.5 and various values of the geometric mean of $F_tV = \exp\{m\}$ are shown in figure 3A, which gives results normalized by the expected number of births for a constant F, which is $N^*F/(1 - FV)$. More variation caused a greater inflation in the number of births, especially with autocorrelation. Equation (A10) is an infinite sum, and was calculated for 1,000 generations for figure 3A.

The second step in the analytical method to approximate the probability of rescue is to find the probability of persistence of the lineage of a single adult mutant, which can be solved using a branching process. The number of mutants surviving after τ generations from a single initial mutant at time 0 is characterized by a probability generating function (PGF)

$$G_\tau(s) = \sum_{j=0}^{\infty} P_\tau(j) s^j \tag{A11}$$

where j is the number of mutants and $P_\tau(j)$ is the probability of j mutants in generation τ after the mutant first appears. In generation 0, there is by assumption one mutant, so $P_0(1) = 1$ (and all other probabilities are 0) and $G_0(s) = s$. In the first generation, this individual gives rise to a Poisson distributed number of offspring. The probability generating function (PGF) for a Poisson distribution with mean R is $f(s) = \exp\{R(s-1)\}$.

The population PGF at generation $\tau + 1$ is found by replacing s in the population PGF at generation τ by the PGF of the number of surviving offspring per adult at generation $\tau + 1$. Therefore, the PGFs for the first few generations are

$$G_0(s) = s \tag{A12}$$

$$G_1(s) = \exp\{R_1(s-1)\} \tag{A13}$$

$$G_2(s) = \exp\{R_1[\exp\{R_2(s-1)\}-1]\} \tag{A14}$$

$$G_3(s) = \exp\{R_1[\exp\{R_2(\exp\{R_3(s-1)\}-1)\}-1]\} \tag{A15}$$

…

$$G_{\tau+1}(s) = G_\tau(\exp\{R_{\tau+1}(s-1)\}) \tag{A16}$$

where $R_\tau = F_\tau v$ is the mean number of surviving mutant offspring per mutant adult at generation τ (F_τ is a Gaussian random sequence as described above, except here we are tracking time from the appearance of a mutant). The probability of extinction at generation τ is $G_\tau(0)$. For constant $R_\tau = R$, this would approach a constant, which is the solution of $q = \exp\{R(q-1)\}$. With R_τ varying, the equations must be solved numerically. We generated 10,000 sequences of R_t (the mutant is assumed to arise at the start of the simulation, so t and τ are the same) each 1,000 generations long, and for each found $G_{1000}(0)$ using equations (A12-A16) and averaged these to get the average probability of extinction within 1,000 generations. Subtracting this from 1 gives the probability of persistence. The results are shown in figure 3B, which shows that there is relatively little change in the probability or persistence due to variation, with only a small decrease with increasing σ, a little more with higher ρ.

The product of the expected number of mutants that arise and survive to adulthood in a given generation (equation (A8) or similar equation using (A10)) and the probability of mutant lineage persistence solved using the method in this section gives the per-generation expected number of mutations that arise and persist, assuming that a mutation arising and its lineage persisting are independent. This should be the case with no autocorrelation. In years with a high fecundity, there will be more births and therefore more expected mutants, but the persistence of a mutant lineage depends on the fecundity in generations after the mutant arises, which are

independent of previous fecundities (given no autocorrelation). Given the expected number of mutants that arise with lineages that persist, the probability of adaptation can be calculated only if the distribution of the number of mutants is known. We assumed that the number of mutants with persisting lineages had a Poisson distribution over all runs to calculate the probability of rescue (Martin et al. 2013; figure A14). With this assumption, letting the expected number of mutations that arise the lineages of which persist be M, then the probability of persistence is the probability that a Poisson with this mean is not 0, which is $1 - \exp\{-M\}$. (With no variation, this method is very similar to Orr and Unckless 2008, except that they assume that the mutant fitness is close to 1 and get a closed-form solution. Since this assumption is not true for our parameters and we do not use their approximation for probability of lineage persistence, we get a somewhat lower persistence probabilities when $\sigma_\theta = 0$, e.g., 0.039 compared to 0.054 for $u = 0.0001$ in figure A14B.) The calculated results agree well with the simulation results for low mutation rates and low-to-moderate variation (for which the expected number of mutants was low; figure A14).

With autocorrelation, the probability of a mutant arising and its lineage persisting are not independent, because population sizes (and therefore births and the expected number of mutants) are large during sequences of good years, and in those years mutant lineages are more likely to persist. Also, the production of mutants tends to be more concentrated into fewer populations (the ones that happen to have runs of good years at the beginning of the simulation), so the assumption of a Poisson distribution among populations is less justified because the actual distribution becomes over-dispersed. Thus our analytical predictions have a greater deviation from the simulations with autocorrelation, predicting higher persistence where they differ (figure A14). Our analytical model might overpredict the probability of rescue because the probability of rescue is a concave function of the number of mutants, thus when the number of mutants is

overdispersed, deviations below the mean outweigh deviations above it. This effect was observed in Uecker and Hermission (2016). (Note that the branching process method we employed calculates mutant lineage survival for 1,000 generations, while in the direct simulations, a mutant lineage only had to survive until the end of the 1,000-generation simulation, and could have arisen from a mutation at any time. This should make almost no difference, because mutant lineages arise before non-mutants go extinct, which tends to happen early in the simulations, and because mutant lineages tend either to go extinct quickly or persist indefinitely.)

Population-level polygenic model: Varying fecundity

We also ran simulations of the polygenic model in which we modelled temporal environmental variation by varying the fecundity F_t, which simulates environmental variation that is independent of the selection pressure. Autocorrelated random sequences of F_t were generated by using equations (2.3a–b).

Variation in the mean population fecundity had a qualitatively similar effect on the probability of persistence to that observed for variation in the optimal phenotype. That is, variation in fecundity was detrimental in low-extinction-risk scenarios but beneficial in high-risk ones (figure A15). In general, these effects were amplified with greater degrees of variation and autocorrelation, but, as with variation in the optimal phenotype, there was a decline in the probability of persistence even in harsh environments when the magnitude of variation became very large. In this case, however, this decline occurs simply because large fluctuations in fecundity can result in years with very low birth rates, which lead to rapid declines in population size. Furthermore, as with variation in the optimal phenotype, the environmental conditions

immediately following the step change had the greatest influence on the outcome of simulations (figure A16).

Methods for individual-based simulations with varying fecundity can be found above in the section *Polygenic individual-based simulation methods*. Results of those simulations are seen in figure A15E,F. Note that in these individual-based simulations with variation in fecundity the effect of variation on evolutionary rescue were minor and, as with variation in the optimal phenotype, we did not see any benefit in high-extinction-risk scenarios when fluctuations were uncorrelated.

Polygenic model: Population-level statistical prediction

Our goal was to evaluate how well the mean optimal phenotype of generations t_i to t_j (hereafter $M_{i,j}$) predicted whether or not the population size would drop below the critical population size N_c during the run of a simulation (1,000 generations). To do this we ran 1,000 runs of the simulation with the parameter values: $\mu_\theta = 4.3$, $\sigma_\theta = 0.6$, $\rho = 0.9$, $N^* = 10{,}000$, $N_c = 100$, $\mu_F = 1.2$, $\omega^2 = 10$, $P = 1$, $G = 0.5$.

We then fit the simulation results to a generalized linear model (GLM) with a binomial distribution and logit link function. Our independent variable was $M_{i,j}$ (for $M_{1,20}$, $M_{21,40}$ and $M_{41\text{-}60}$) and our response variable was whether or not the population dropped below N_c during the course of the simulation. We then calculated McFadden's R^2 values using the package *pscl* (Jackman 2017) in R 3.63 (R Core Team 2020). McFadden's R^2 is a measure of fit which compares a model with just the intercept (null model) to a model with all the parameters (full model). Specifically,

$$\text{McFadden's } R^2 = 1 - \frac{\log \text{likelihood (full model)}}{\log \text{likelihood (null model)}}$$

(Long 1997). Larger values of McFadden's R^2 indicate a better model fit.

To evaluate model predictability, we then ran an additional 1,000 runs of the simulation with the same parameter values. Using the function *predict* in R 3.63 (R Core Team 2020), we predicted the results of the second 1,000 runs of the simulation using the GLM that was fit to the first 1,000 runs of the simulation. This output probabilities that any given simulation run would drop below N_c given $M_{i,j}$. We used a 0.5 decision boundary such that if the GLM predicted that the probability of the run going below N_c was greater than 50%, we recorded the model as predicting extinction for that run of the simulation. We then compared the prediction of the GLM to the actual results of the second 1,000 runs of the simulation to obtain our estimate of prediction accuracy.

Citations:

Jackman S. 2010 pscl: Classes and methods for R. Developed in the Political Science Computational Laboratory, Stanford University. Department of Political Science, Stanford University, Stanford, CA. R package version 1.03. 5. *http://www. pscl. stanford. edu/*.

Long JS. 1997. Regression models for categorical and limited dependent variables (Vol. 7). *Advanced quantitative techniques in the social sciences*.

Martin G, Aguilée R, Ramsayer J, Kaltz O, Ronce O. 2013 The probability of evolutionary rescue: towards a quantitative comparison between theory and evolution experiments. *Phil. Trans. R. Soc. B* **368**, 20120088. (doi:10.1098/rstb.2012.0088)

Orr HA, Unckless RL. 2008. Population extinction and the genetics of adaptation. *Am. Nat.* ***172***: 160-9.

R Core Team 2020. R: A language and environment for statistical computing. R Foundation for Statistical Computing, Vienna, Austria. URL https://www.R-project.org/

Uecker H, Hermisson J. 2016. The role of recombination in evolutionary rescue. *Genetics* ***202***, 721–732. (doi: 10.1534/genetics.115.180299).

Supplementary Figures

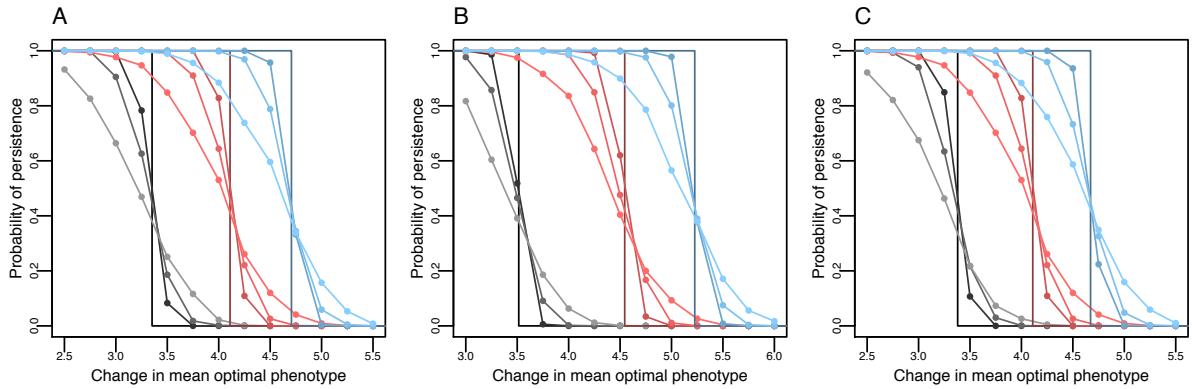

Figure A1. Sensitivity analyses for the polygenic population-level model. For all parameter values, the plots show four different degrees of variation in the optimal phenotype ($\sigma_\theta = 0.0$, $\sigma_\theta = 0.2$, $\sigma_\theta = 0.4$, and $\sigma_\theta = 0.8$) with lighter shades indicating greater degrees of variation. (A) Three different values for the critical population size, N_c, below which the population is considered extinct: N_c = 1,000 (grey), N_c = 100 (red), and N_c = 10 (blue). (B) Three different

values for the strength of stablizing selection: $\omega^2 = 5$ (grey), $\omega^2 = 15$ (red), $\omega^2 = 25$ (blue). (C) Three different values for the additive genetic variance: $G = 0.25$ (grey), $G = 0.5$ (red), $G = 0.75$ (blue). Each point represents the proportion of 1,000 runs of the simulations in which the population did not drop below the critical population size N_c at any point of the simulation. Unless otherwise stated, the parameter values were: $N^* = 10{,}000$, $N_c = 100$, $\mu_F = 1.2$, $\omega^2 = 10$, $P = 1$, $G = 0.5$, and $\rho = 0.9$.

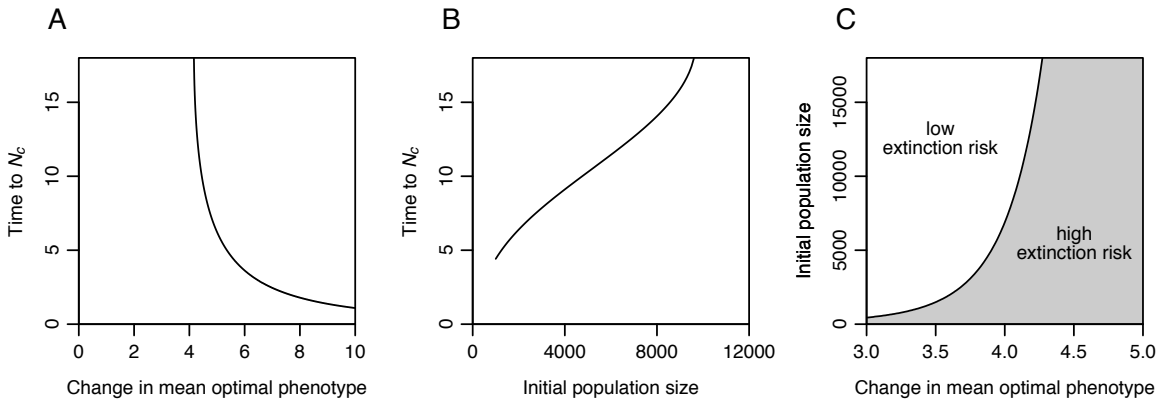

Figure A2. Examples of how baseline extinction risk is affected by the change in the mean optimal phenotype (with no variation after the change) and the initial population size in the polygenic population-level model. (A) and (B) show the number of generations until the population reaches the critical population size N_c, below which the population is assumed to go extinct, as given by equation (3.1). If the time to N_c is undefined, the population never drops below N_c and thus rescue occurs without variation, which we consider here to be a low-extinction-risk scenario. We consider finite times to N_c to be a high-extinction-risk scenario. (C)

Plot showing parameter space of low- and high-extinction-risk scenarios. Parameter values in all panels were: $N_c = 100$, $\mu_F = 1.2$, $\omega^2 = 10$, $P = 1$, $G = 0.5$. In (A), $N^* = 10{,}000$. In (B), $\mu_\theta = 4.1$.

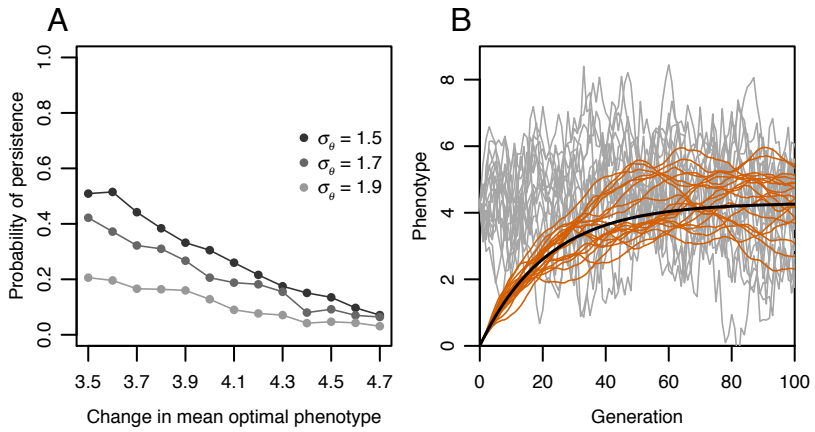

Figure A3. Results of the population-level polygenic models for high levels of variation in the optimal phenotype. (A) Shows results for three different degrees of variation (σ_θ). Each point represents the proportion of 1,000 runs of the simulations in which the population did not drop below the critical population size N_c at any point of the simulation. (B) Shows examples of phenotypic evolution in a highly variable environment ($\sigma_\theta = 1.5$). The optimum phenotype with mean $\mu_\theta = 4.3$ (grey lines) and mean phenotype (orange lines) from 20 randomly selected runs of the simulation are plotted. The parameter values were: $N^* = 10{,}000$, $N_c = 100$, $\mu_F = 1.2$, $\omega^2 = 10$, $P = 1$, $G = 0.5$, and $\rho = 0.9$.

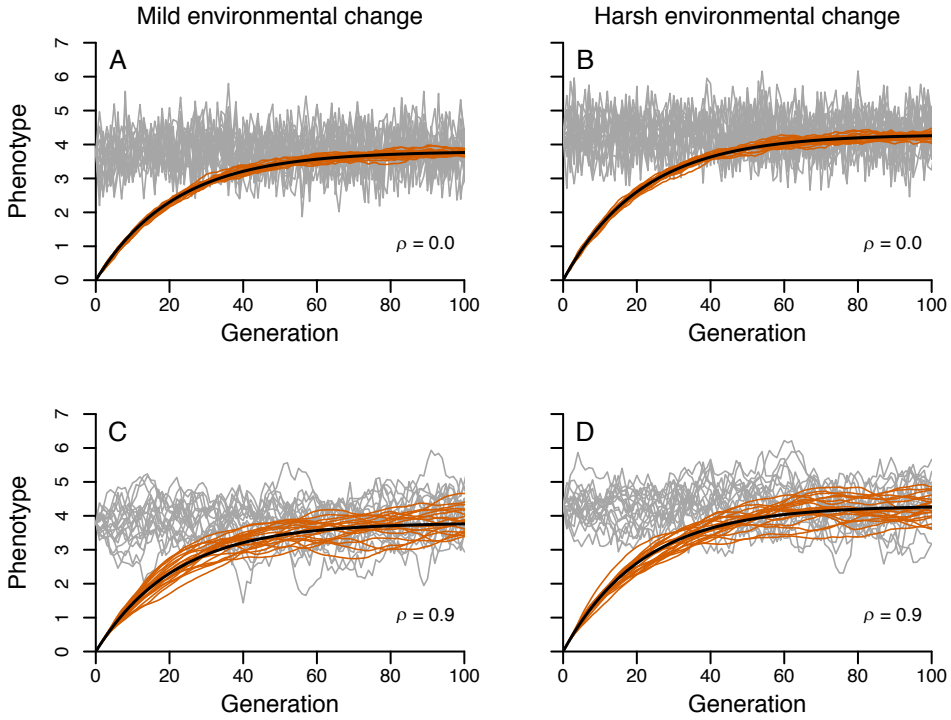

Figure A4. Phenotypic evolution in the population-level polygenic models following an abrupt change in the optimal phenotype. Each panel shows the optimum phenotype (grey lines) and mean phenotype (orange lines) for 20 randomly selected runs of the simulation. (A) and (B) show results for uncorrelated fluctuations in the optimal phenotype ($\rho = 0.0$) and (C) and (D) show results for autocorrelated fluctuations in the optimal phenotype ($\rho = 0.9$). In all panels, $\sigma_\theta = 0.6$, $N_c = 100$, $\mu_F = 1.2$, $\omega^2 = 10$, $P = 1$, $G = 0.5$. In (A) and (C), $\mu_\theta = 3.8$ and in (B) and (D), $\mu_\theta = 4.3$.

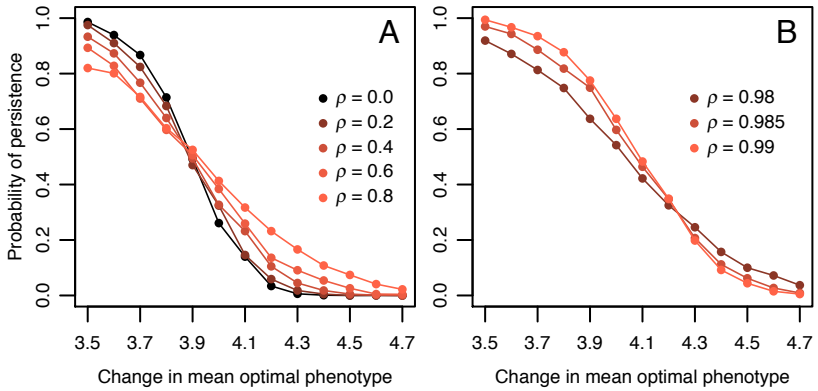

Figure A5. The effect of autocorrelation in fluctuations of the optimum phenotype on the probability of persistence in the population-level polygenic models. (A) shows that for most values, increasing the degree of autocorrelation (ρ) increased both the positive and negative effects of fluctuations of the optimum phenotype. However, (B) shows that at high levels of autocorrelation ($\rho > 0.98$) increasing the degree of autocorrelation decreased the positive and negative effects of fluctuations of the optimum phenotype. Each point represents the proportion of 1,000 runs of the simulation in which the population did not drop below the critical population size N_c at any point of the simulation. Parameter values in both panels are $\sigma_\theta = 0.8$, $N_c = 100$, $\mu_F = 1.2$, $\omega^2 = 10$, $P = 1$, $G = 0.5$.

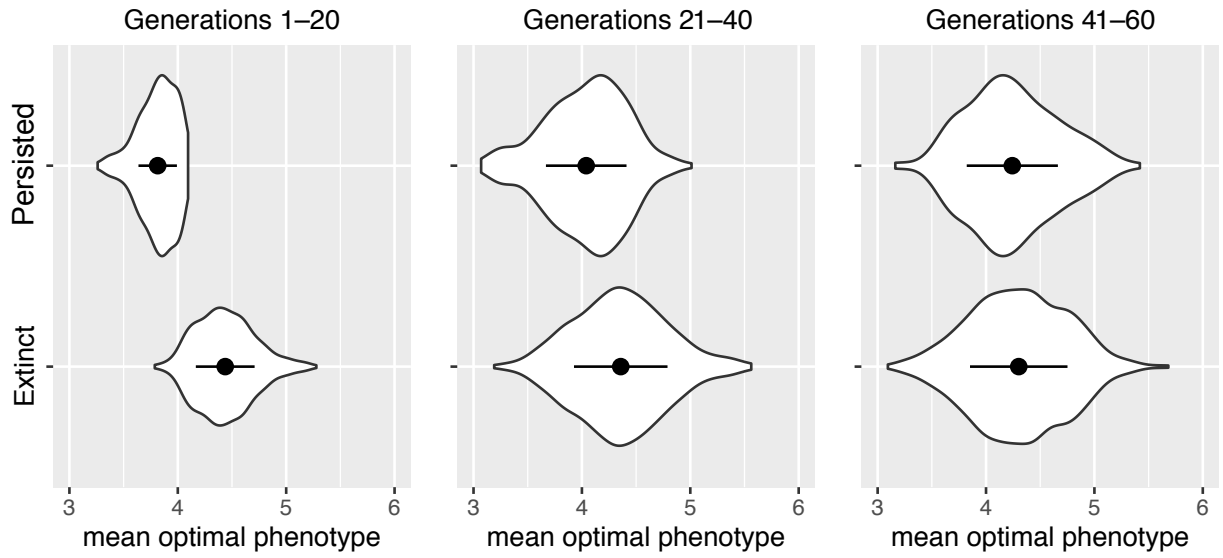

Figure A6. Violin plots showing the mean optimal phenotype from generation *i* to *j* for populations that went extinct and populations that persisted in runs of the polygenic population-level simulations with fluctuations in the optimal phenotype. Each panel shows the results of 1,000 runs of the simulation. The mean (black circle) and standard deviation (black bar) are shown for each group. Populations were recorded at 'Extinct' if the population dropped below the critical population size N_c at any point of the simulation (1,000 generations); otherwise, they were recorded as 'Persisted'. Parameter values were: $N^* = 10{,}000$, $N_c = 100$, $\mu_\theta = 4.3$, $\mu_F = 1.2$, $\omega^2 = 10$, $P = 1$, $G = 0.5$, $\sigma_\theta = 0.6$, $\rho = 0.9$.

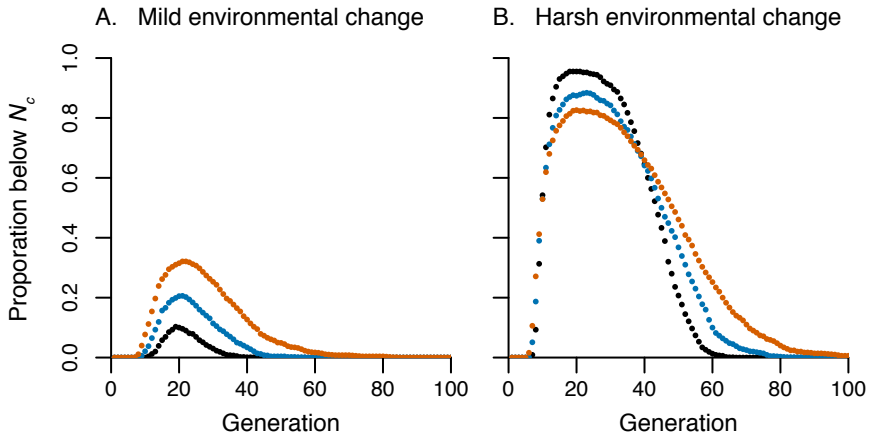

Figure A7. Proportion of 1,000 runs of the population-level polygenic simulation in which the population size is below N_c at a given number of generations (the abscissa) after an abrupt environmental change. Three different degrees of variation are shown in each panel: $\sigma_\theta = 0.4$ (black), $\sigma_\theta = 0.6$ (blue), $\sigma_\theta = 0.8$ (orange). In both panels, $N_c = 100$, $\mu_F = 1.2$, $\omega^2 = 10$, $P = 1$, $G = 0.5$, $\sigma_\theta = 0.6$, and $\rho = 0.9$. In (A), $\mu_\theta = 3.8$ and in (B), $\mu_\theta = 4.3$.

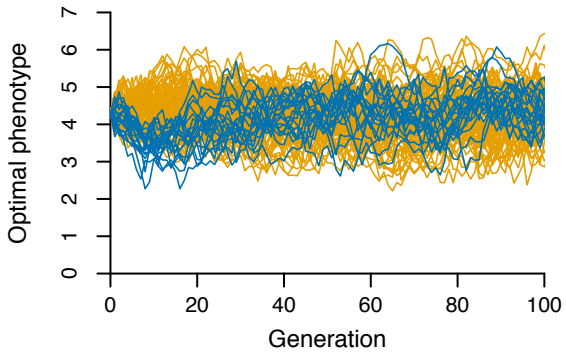

Figure A8. Optimal phenotype values for the first 100 generations after environmental change in 100 randomly selected runs of the population-level polygenic simulations. Light orange lines denote runs in which the population dropped below the critical population size N_c at some point in the simulation and dark blue lines denote runs in which the population never dropped below N_c. Note that in the first 20 generations the dark blue lines are on average lower than the light orange lines. Compare with figure A6. Parameters were: N^* = 10,000, N_c = 100, $\mu_\theta = 4.3$, $\mu_F = 1.2$, $\omega^2 = 10$, P = 1, G = 0.5, $\sigma_\theta = 0.6$, $\rho = 0.9$.

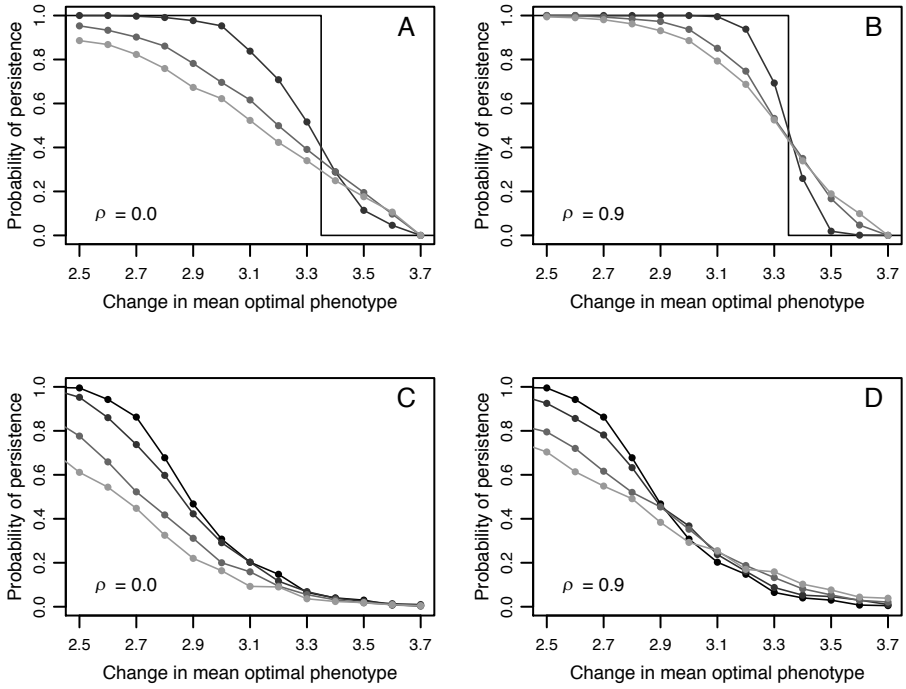

Figure A9. Comparison of population-level (A and B) and individual-based simulations (C and D) for the polygenic model with variation in the optimal phenotype. In (A) and (B), each point represents the proportion of 1,000 runs of the simulations in which the population did not drop below the critical population size N_c at any point of the simulation and in (C) and (D) each point represents the proportion of 800 runs of the simulations in which populations persisted. The left panels (A and C) show results for uncorrelated fluctuations in the optimal phenotype ($\rho = 0$) and the right panels (B and D) show results for autocorrelated fluctuations in the optimal phenotype ($\rho = 0.9$). Each panel shows results for different degrees of fluctuations in the optimal phenotype: $\sigma_\theta = 0.0$, $\sigma_\theta = 0.4$, $\sigma_\theta = 0.8$, and $\sigma_\theta = 1.0$ with lighter shades of grey indicating greater degrees of variation. In all panels, $N^* = 1{,}000$, $\mu_F = 1.2$, and $\omega^2 = 1$. Additional parameters for (A) and (B) were $N_c = 100$, $P = 1$, $G = 0.5$, and in (C) and (D) $K = 250$.

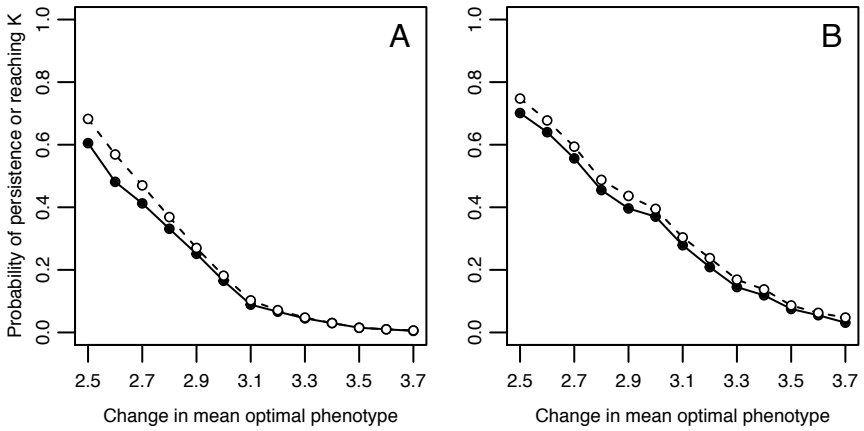

Figure A10. Effect of density regulation in the polygenic individual-based simulations. Each point represents the proportion of 800 runs of the simulation in which the population either persisted until the end of the simulation (black circles) or had greater than *K* adults at any point in the simulation (white circles). (A) shows uncorrelated fluctuations in the optimal phenotype ($\sigma_\theta = 1.0$, $\rho = 0.0$) and (B) shows autocorrelated fluctuations in the optimal phenotype ($\sigma_\theta = 1.0$, $\rho = 0.9$). Parameters values were: $N^* = 1{,}000$, $\mu_F = 1.2$, $\omega^2 = 1$, and $K = 250$.

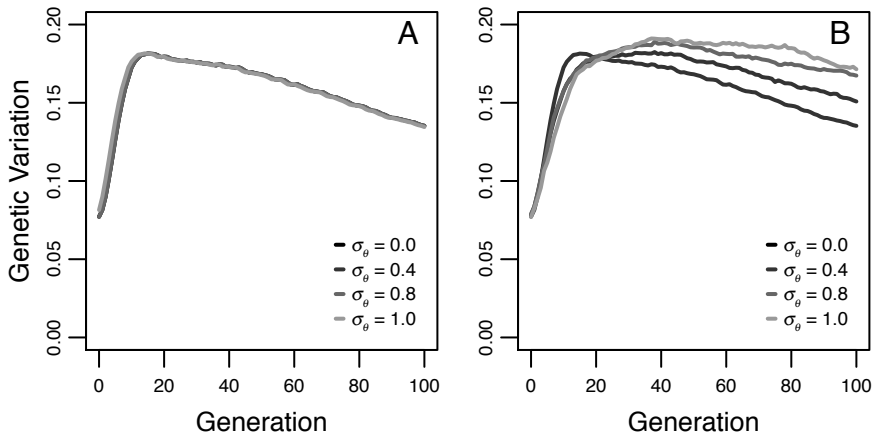

Figure A11. Effect of fluctuations in the optimal phenotype on additive genetic variation in the polygenic individual-based simulations. Lines show the mean additive genetic variation of 800 runs of the simulation with either uncorrelated (A; $\rho = 0.0$) or positively autocorrelated (B; $\rho = 0.9$) fluctuations in the optimal phenotype. Lighter shades of grey indicate greater degrees of variation in the optimal phenotype (σ_θ). Additive genetic variation was calculated at the beginning of each generation before individuals were subject to viability selection. It was calculated by calculating the variance among individuals' genotypic values. Recall that in our population-level polygenic models, additive genetic variance was assumed to be temporally constant. Parameters values were: $N^* = 1{,}000$, $\mu_F = 1.2$, $\omega^2 = 1$, and $K = 250$.

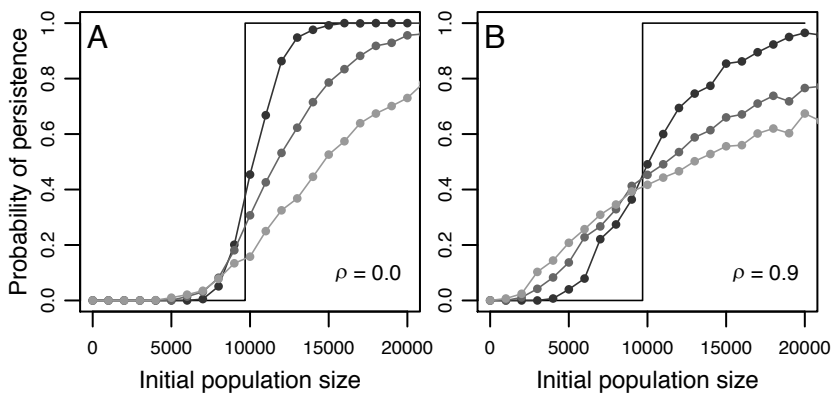

Figure A12. The probability of persistence in the population-level polygenic model for different initial population sizes with either uncorrelated (A; $\rho = 0$) or positively autocorrelated (B; $\rho = 0.9$) fluctuations in the optimal phenotype. Each panel shows results for different degrees of fluctuations in the optimal phenotype: $\sigma_\theta = 0.0$, $\sigma_\theta = 0.2$, $\sigma_\theta = 0.4$, and $\sigma_\theta = 0.8$ with lighter shades of grey indicating greater degrees of variation. Each point represents the proportion of 1,000 runs of the simulations in which the population never dropped below the critical population size N_c. Parameter values were: $\mu_\theta = 4.1$, $N_c = 100$, $\mu_F = 1.2$, $\omega^2 = 10$, $P = 1$, $G = 0.5$.

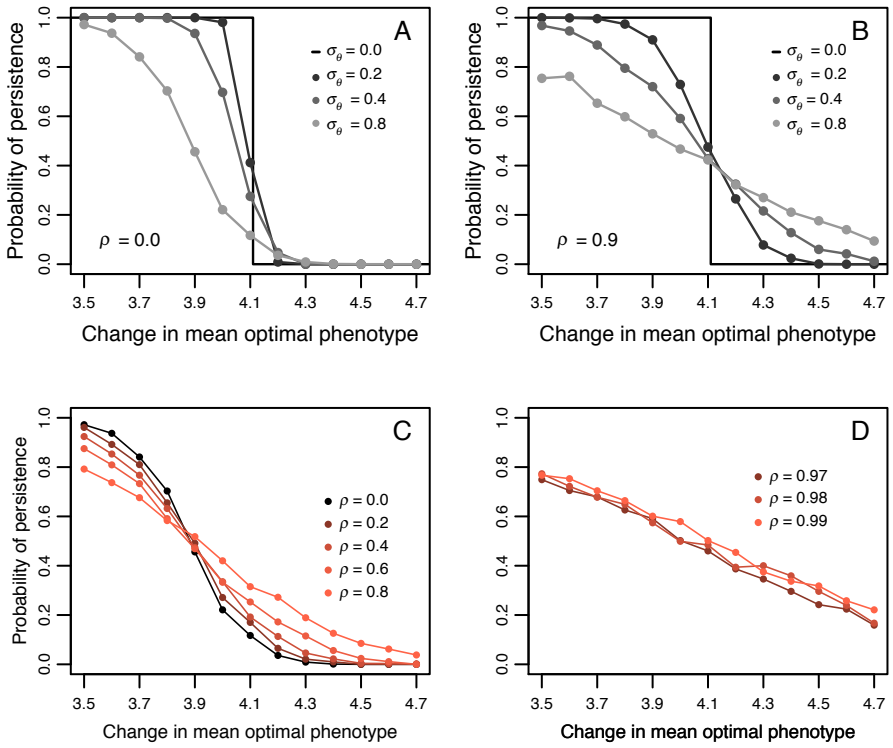

Figure A13. Population-level polygenic model with the optimal phenotype of the first generation after the environmental change being a random Gaussian variable with mean μ_θ and variance σ_θ^2. This differs from the results presented in the main text (and elsewhere in the supplemental material) in which the optimal phenotype of the first generation after the environmental change was always μ_θ. (A) and (B) show the effects of increasing the magnitude of variation in the optimal phenotype σ_θ^2 without (A; $\rho = 0$) and with (B; $\rho = 0.9$) autocorrelation. (A) and (B) are comparable to figure 2 in the main text. (C) and (D) show the results of increasing autocorrelation, which is comparable to figure A4. For (C) and (D) $\sigma_\theta^2 = 0.8$. In all panels, each point represents the proportion of 1,000 runs of the simulation in which the population did not

drop below the critical population size N_c at any point of the simulation. Parameter values in both panels are $N_c = 100$, $\mu_F = 1.2$, $\omega^2 = 10$, $P = 1$, $G = 0.5$.

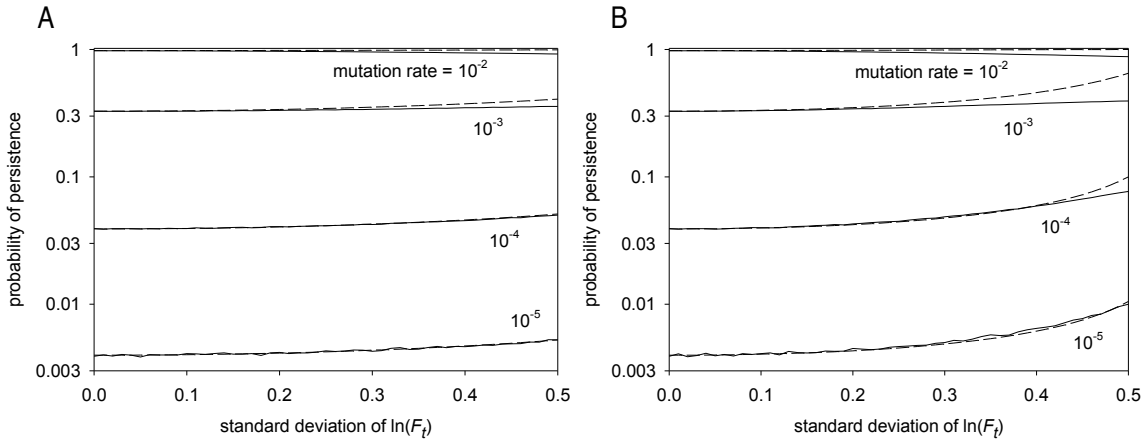

Figure A14. Agreement between simulation results (solid lines) and our analytical approximation (dashed lines) for the monogenic model. The solid lines are generated from simulations with 1,000,000 realizations for each parameter set (at intervals of 0.01 on the abscissa) as in figure 3c (although fecundity here is lower), while the dashed lines are values calculated using the expected number of mutants and probability of mutant lineage persistence, and assuming a Poisson distribution of mutants among populations. (A) shows uncorrelated variation and (B) shows autocorrelated variation with $\rho = 0.5$. Note that the ordinate is on a logarithmic scale. Parameter values were: $N^* = 100$, geometric mean $F_t = 3$, $V = 0.2$, $v = 0.5$.

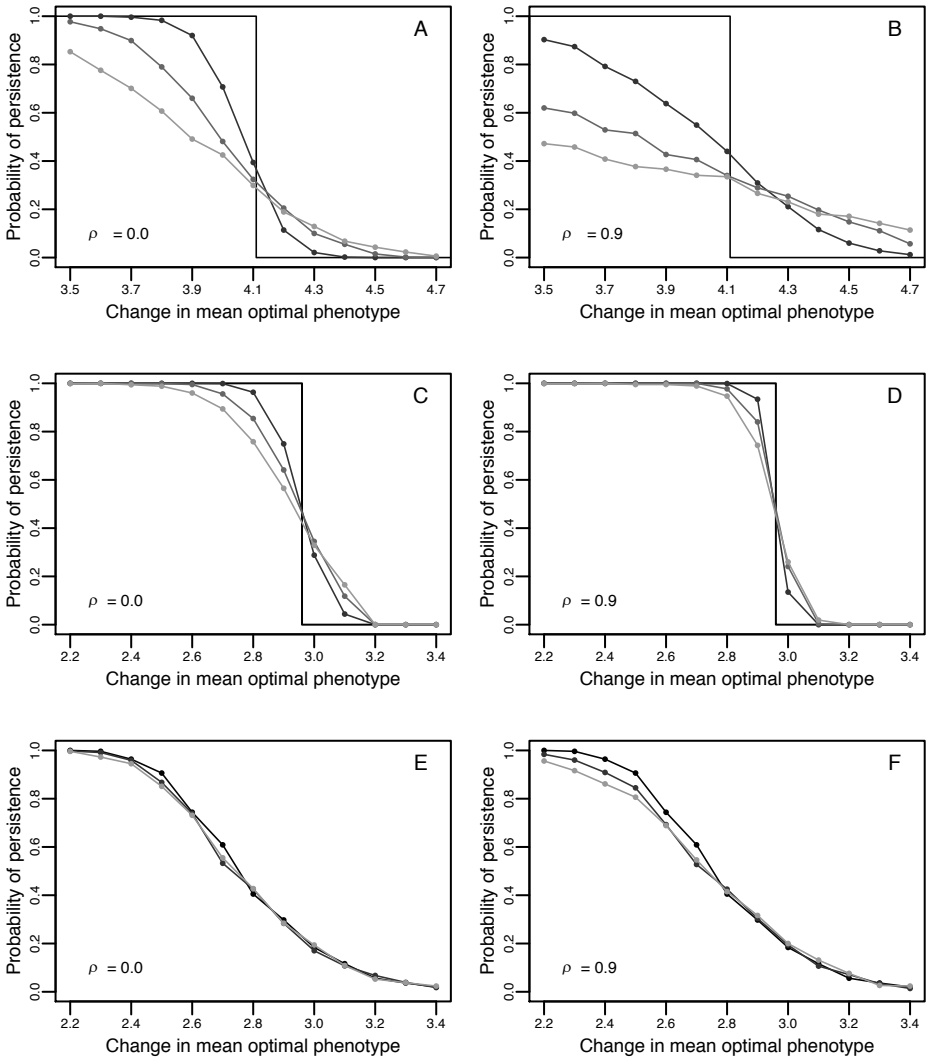

Figure A15. The effects of variation in fecundity in the polygenic model on the probability of persistence following a sudden environmental change. The left column (A,C,E) shows results for uncorrelated fluctuations (ρ = 0.0) and the right column (B,D,F) shows results for positively autocorrelated fluctuations (ρ = 0.9). (A) and (B) show results of the population-level simulations with a large initial population size (10,000) and weak stabilizing selection ($\omega^2 = 10$). (C) and (D) show results of the population-level simulations with a smaller initial population size (1,000) and stronger stabilizing selection ($\omega^2 = 1$). (E) and (F) show results of

the individual-based simulations with an initial population size of 1,000 and stabilizing selection of $\omega^2 = 1$. In (A), (B), (C), and (D) each point represents the proportion of 1,000 runs of the simulations in which the population did not drop below the critical population size N_c at any point of the simulation and in (E) and (F) each point represents the proportion of 800 runs of the simulations in which populations persisted. In all plots, lighter shades of grey indicate greater variation in fecundity (σ_F). In the population-level simulations (A,B,C,D), the degrees of variation shown are $\sigma_F = 0$, $\sigma_F = 0.2$, $\sigma_F = 0.3$, and $\sigma_F = 0.4$. In the individual-based simulations, the degrees of variation shown are $\sigma_f = 0.0$, $\sigma_f = 0.35$, and $\sigma_f = 0.4$. Additional parameters for (A) and (B) were $\mu_F = 1.2$, $N_c = 100$, $P = 1$, $G = 0.5$. Additional parameters for (C) and (D) were $\mu_F = 3.5$, $N_c = 200$, $P = 1$, $G = 0.5$. In (E) and (F) $\mu_F = 3.5$ and $K = 250$.

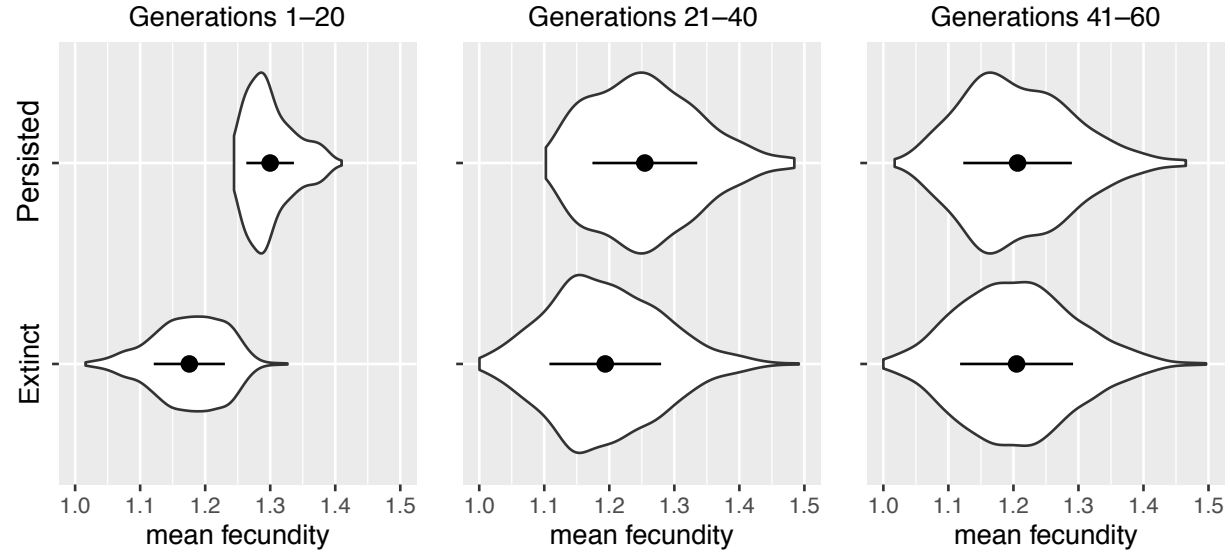

Figure A16. Violin plots showing the mean fecundity from generation *i* to *j* for populations that went extinct and populations that persisted in runs of the polygenic population-level simulations

with fluctuations in fecundity. Each panel shows the results of 1,000 runs of the simulation. The mean (black circle) and standard deviation (black bar) are shown for each group. Populations were recorded as 'Extinct' if the population dropped below the critical population size N_c at any point of the simulation (1,000 generations); otherwise, they were recorded as 'Persisted'. Parameter values were: initial population size = 10,000, $N_c = 100$, $\mu_\theta = 4.3$, $\mu_F = 1.2$, $\omega^2 = 10$, $P = 1$, $G = 0.5$, $\sigma_\theta = 0.1$, $\rho = 0.9$.